Circulation Reports
Circ Rep 2019; 1: 333–341
doi:10.1253/circrep.CR-18-0024

ORIGINAL ARTICLE
Imaging

Prediction of Cardiac Resynchronization Therapy Response in Dilated Cardiomyopathy Using Vortex Flow Mapping on Cine Magnetic Resonance Imaging

Risako Nakao, MD; Michinobu Nagao, MD, PhD; Kenji Fukushima, MD, PhD; Akiko Sakai, MD; Eri Watanabe, MD, PhD; Masateru Kawakubo, PhD; Shuji Sakai, MD, PhD; Nobuhisa Hagiwara, MD, PhD

Background: We investigated the association between left ventricle ejection fraction (LVEF) and vortex flow (VF), and whether cardiac resynchronization therapy (CRT) response can be predicted using VF mapping (VFM) in patients with dilated cardiomyopathy (DCM).

Methods and Results: Cardiac magnetic resonance imaging data for 20 patients with heart failure (HF) with LVEF ≥40% and 25 patients with DCM with LVEF <40%, scheduled for CRT, were retrospectively analyzed. The maximum VF (MVF) on short-axis, long-axis and 4-chamber LV cine imaging were calculated using VFM. Summed MVF was used as a representative value for each case and was significantly greater for patients with DCM than for patients with HF with LVEF ≥40% (25.2±19.2% vs. 12.1±15.4%, P<0.005). Summed MVF was significantly greater for CRT responders (n=12, 35.8±22.7%) than for non-responders (n=13, 15.8±8.7%, P=0.04) during the mean follow-up period of 38.4 months after CRT. Patients with summed MVF ≥31.3% had a significantly higher major adverse cardiac event-free rate than those with MVF <31.3% (log-rank=4.51, P<0.05).

Conclusions: On VFM analysis, LV VF interrupted efficient ejection in HF. Summed MVF can predict CRT response in DCM.

Key Words: Cardiac resynchronization therapy; Dilated cardiomyopathy; Magnetic resonance imaging; Steady-state free precession

Cardiac resynchronization therapy (CRT) is 1 of the effective therapies for advanced heart failure (HF) with mechanical dyssynchrony. The 2016 ESC guidelines recommend CRT implantation according to the following parameters. CRT is recommended for symptomatic patients in sinus rhythm, with wide QRS duration (≥120 ms), with left bundle branch block (LBBB) QRS morphology, and with left ventricle ejection fraction (LVEF) ≤35%.[1] Although these parameters have been considered to be parallel to the progression of dyssynchrony, approximately 20–30% of patients were non-responders to CRT. In order to predict response to CRT, several dyssynchrony indexes derived from echocardiography have been proposed, but neither parameter is a certain predictor of CRT.

Interventricular vortex dynamics may have an important role in cardiac hemodynamics. Vortex flow mapping (VFM) using conventional cine cardiac magnetic resonance imaging (CMR) that enables quantification and visualization of turbulent flow in the cardiac cavity and the great vessels, has recently been developed. On VFM analysis, vortex flow (VF) in Fontan circulation has been shown to be associated with the development of Fontan-associated liver disease,[2] and with supraventricular arrhythmia in adolescent patients with congenital single ventricle.[3] We hypothesized that mechanical dyssynchrony causes VF to disrupt efficient output; therefore, CRT response may be associated with the occurrence of LV VF. The aims of the present study were to investigate the relationship between efficient LV ejection and VF, and whether CRT response could be predicted on VFM analysis in patients with dilated cardiomyopathy (DCM).

Methods

Patients

This retrospective cohort study was approved by the institutional research ethics board and involved 20 HF patients with LVEF ≥40% and 25 DCM patients with LVEF <40% who were scheduled for CRT between January 2010 and December 2016. All patients underwent CMR, cardiac catheterization, transthoracic echocardiography, 12-lead electrocardiogram (ECG), and clinical examination at the same

Received December 7, 2018; revised manuscript received June 10, 2019; accepted June 17, 2019; J-STAGE Advance Publication released online July 26, 2019 Time for primary review: 52 days

Department of Cardiology (R.N., A.S., E.W., N.H.), Department of Diagnostic Imaging and Nuclear Medicine (M.N., K.F., S.S.), Tokyo Women's Medical University, Tokyo; Department of Health Sciences, Faculty of Medical Sciences, Kyushu University, Fukuoka (M.K.), Japan

N.H. is a member of *Circulation Reports*' Editorial Team.

Mailing address: Michinobu Nagao, MD, PhD, Department of Diagnostic Imaging and Nuclear Medicine, Tokyo Women's Medical University, 8-1 Kawada-cho, Shinjuku-ku, Tokyo 162-8666, Japan. E-mail: nagao.michinobu@twmu.ac.jp

ISSN-2434-0790

Table 1. Subject Characteristics

	CRT group (n=25)	LVEF ≥40% group (n=20)	P-value
Clinical characteristics			
Age (years)	59.2±16.0	48.1±15.3	0.016
Male	24 (96)	12 (60)	0.0032
NYHA I/II/III	1/11/13	20/0/0	
Paroxysmal AF	4 (16)	1 (5)	0.36
Diagnosis			
DCM	25 (100)	11 (55)	
Others	0 (0)	9 (45)	
MR parameters			
LVEF (%)	16.2±7.8	44.5±4.5	<0.001
LVEDV (mL)	298.2±160.0	132.8±36.8	<0.001
Vortex flow mapping			
MVF (short-axis) (%)	6.4±8.0	3.2±7.6	0.018
MVF (long-axis) (%)	7.8±9.6	4.0±4.7	0.049
MVF (4-chamber) (%)	11.0±12.8	4.9±7.5	0.0088
Summed MVF (%)	25.2±19.2	12.1±15.4	0.0027

Data given as mean±SD or n (%). AF, atrial fibrillation; CRT, cardiac resynchronization therapy; DCM, dilated cardiomyopathy; LVEDV, left ventricular end-diastolic volume; LVEF, left ventricular ejection fraction; MR, magnetic resonance; MVF, maximum vortex flow; NYHA, New York Heart Association.

time as part of their routine follow-up, and their clinical history and New York Heart Association (NYHA) functional class were collected from the medical records. The reference cohort was defined as those having no history of significant clinical events such as arrhythmias or HF. For patients scheduled for CRT, the presence or absence of LV dyssynchrony was determined on echocardiography and CMR. The median time from CMR to CRT implantation was 12 days. The characteristics of the patients in the CRT group and LVEF ≥40% group are summarized in **Table 1**. In the LVEF ≥40% group, 11 patients had a clinical diagnosis of DCM, while 9 patients did not (arrhythmia, n=5: PVC, nsVT, paroxysmal AF, atrial tachycardia, and Brugada syndrome; hypertrophic cardiomyopathy, n=1; ventricular septal defect, n=1; and 2 patients underwent CMR to rule out myocardial damage associated with scleroderma).

Definition of CRT Response

For patients with DCM who underwent CRT, blood test for HF markers, ECG, chest radiography, and echocardiography were performed at least every 6 months. CRT response was defined as reduction of LV end-systolic volume (LVESV) ≥15% on echocardiography from before CRT to 6–12 months after CRT.[4] In addition, CRT responders were not hospitalized for decompensated HF during the follow-up period. Non-response was defined as acute decompensated HF (ADHF), including arrhythmias, hemostatic complications (including thromboembolism and hemoptysis), catheterization and/or surgical intervention, and death. Death was defined as sudden when it occurred ≤1 h after acute symptoms, and as secondary to HF when it occurred after progressively worsening HF. Follow-up data were obtained from hospital records. In cases of multiple events, the censoring event was the first sequential event.

CMR

Twenty-three patients (including 16 patients with CRT), were examined using a 1.5-T MRI scanner (Gyroscan ACS-NT, Philips Medical Systems, Best, the Netherlands) between January 2010 and March 2014, and 12 patients (including 9 patients with CRT) using a 3.0-T MRI scanner (Ingenia, Philips Medical Systems, Best, the Netherlands) between April 2014 and December 2016 with a 4-element phased-array coil in the supine position with breath-holds during expiration and ECG gating.

Cine images were acquired using cine-balanced turbo field-echo sequences (repetition time, 2.8 ms; echo time, 1.4 ms; flip angle, 45°; slice thickness, 8 mm; field of view, 380 mm; matrix size, 176×193; SENSE factor 2). There were 20 phases per cardiac cycle, resulting in a mean temporal resolution of 45 ms. LV end-diastolic volume (LVEDV) and LVESV were analyzed semi-automatically at the basal to apical levels using LV short-axis (SA) cine images, followed by manual correction with available software (Ziostation 2; Ziosoft, Tokyo, Japan). End-diastolic and end-systolic phases were identified visually on those images with the largest and smallest LV cavity areas, respectively.

VFM Analysis

Based on the voxel and feature tracking methods, we modified the myocardial strain analysis for cine-tagging using existing software (Ziostation 2; Ziosoft)[5,6] and developed a VFM that enables quantification and visualization of turbulent flow. On conventional 2-D cine imaging with steady-state free precession or balanced turbo field-echo sequences, a dark flow artifact is often seen in an enlarged LV, which is caused by spins moving within an inhomogeneous magnetic field.[7,8] In the dilated LV, the turbulent flow is a result of a mixture of LV inflow by non-unified LV wall motion. The advantage of VFM is that it enables quantification of the area and depth of the dark flow artifact by tracking each voxel, followed by automatic extraction of the voxel movement occurring throughout a cardiac cycle.

First, cine imaging with the maximum cross-section of the LV on SA, long-axis (LA), and 4-chamber views was selected. Second, we delineated the contour of the LV cavity

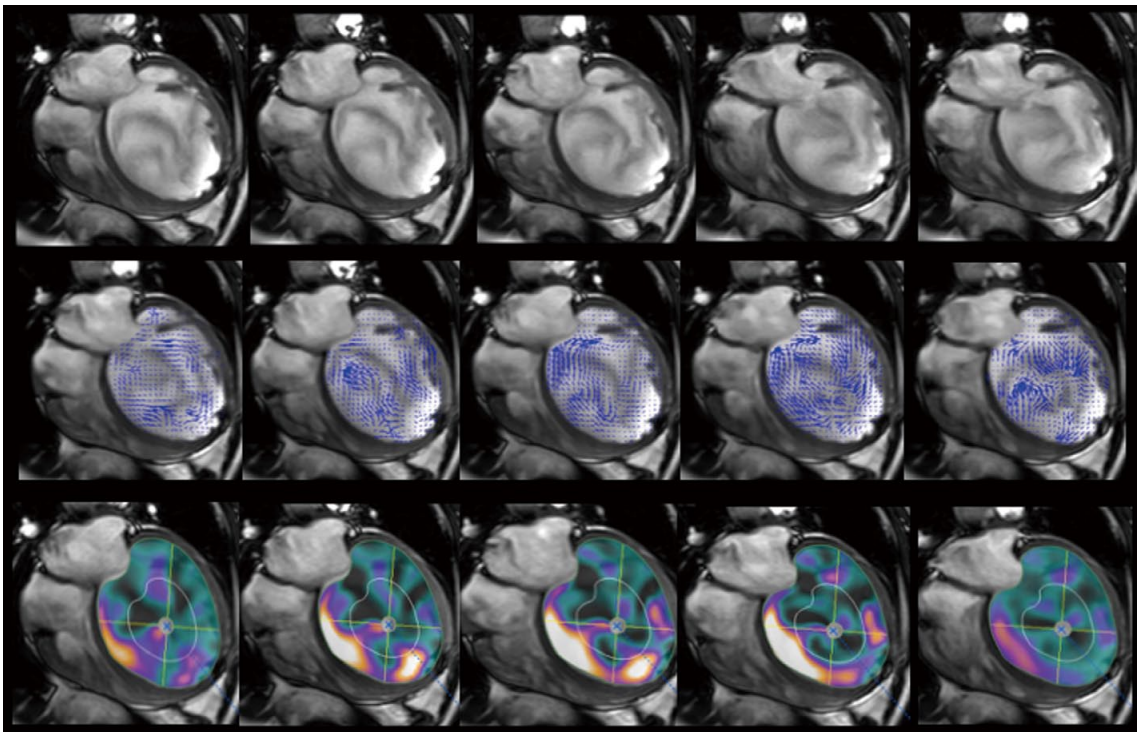

Figure 1. A man in his 40s with dilated cardiomyopathy was classified as a responder 8 months after cardiac resynchronization therapy implantation. (**Upper row**) Four-chamber cine imaging throughout a cardiac cycle (**Left**, early-systole; **Center**, end-systole; **Right**, end-diastole); (**Lower row**) vortex flow map at the same phase. Cine imaging shows multiple dark flow phenomena in the dilated left ventricle. (**Middle row**) Moving dark flow phenomena along the septal wall corresponding to a large vortex with hot colors.

as a region of interest (ROI) and determined the center of the long and short diameter of the LV on the initial frame of the cine image. Third, VFM automatically tracked all pixels in the ROI and calculated the pixel movement for the ROI at each phase during the total pixel movement throughout a cardiac cycle. The vector of pixel movement is resolved into circumferential and radial components. Movement in the circumferential direction is defined as VF. The magnitude of VF is obtained from the following equation:

$$VF\ (\%)=D(t)/D(1),$$

where D(t) is the distance moved by the voxel at time t, and D(1) is the total distance moved by the voxel throughout a cardiac cycle.

The highest MVF was used as the representative value for each case. Summed MVF for the 3 views (SA, LA, and 4-chamber view) was also used. On the VFM, high VF is shown in hot colors, and low VF or stagnation in cold colors (**Figures 1**,**2**).

Identification of Dyssynchrony

CMR-Feature Tracking (CMR-FT) CMR-FT-derived strain analysis was performed using dedicated software (Vitrea, Canon Medical Systems, Tochigi, Japan). The same SA and 4-chamber cine images used for VFM were used for strain measurements. First, endocardial and epicardial borders were manually drawn in the end-diastolic frame. Papillary muscles were excluded from the endocardial contour. These were then automatically propagated through the cardiac cycle by matching individual patterns that represent anatomical structures.[9] Second, mid-LV SA and 4-chamber cine images were divided into 6 myocardial segments. Circumferential strain for the mid-LV SA and longitudinal strain for the 4-chamber view were calculated for each segment. Based on the cross-correlation analysis of the strain-time curve, the temporal delay was calculated between the septal and lateral time curves by shifting 1 curve in time relative to the other curve and calculating the normalized correlation between the curves for each time shift. The time shift between the 2 curves that resulted in the maximum correlation value was defined as the temporal delay between the 2 strain-time curves.[10,11] In the case of faulty propagation, the track line can be re-adapted to the endocardial border. Then, the software propagates a new track line based on the manually made corrections. **Figure 3** shows an example of CMR-FT.

Echocardiography We measured interventricular and intraventricular dyssynchrony index using echocardiography based on previous studies.[12–14] The time difference between the LV pre-ejection period (PEP) and right ventricular PEP was measured for interventricuar wall motion delay (IVMD). IVMD >40 ms was defined as positive for interventricular dyssynchrony. The speckle tracking radial strain delay index was used as an estimate of intraventricular dyssynchrony. The time-radial strain curve on SA view of the LV at the papillary muscle level was semi-automatically drawn using the speckle tracking method. The time difference

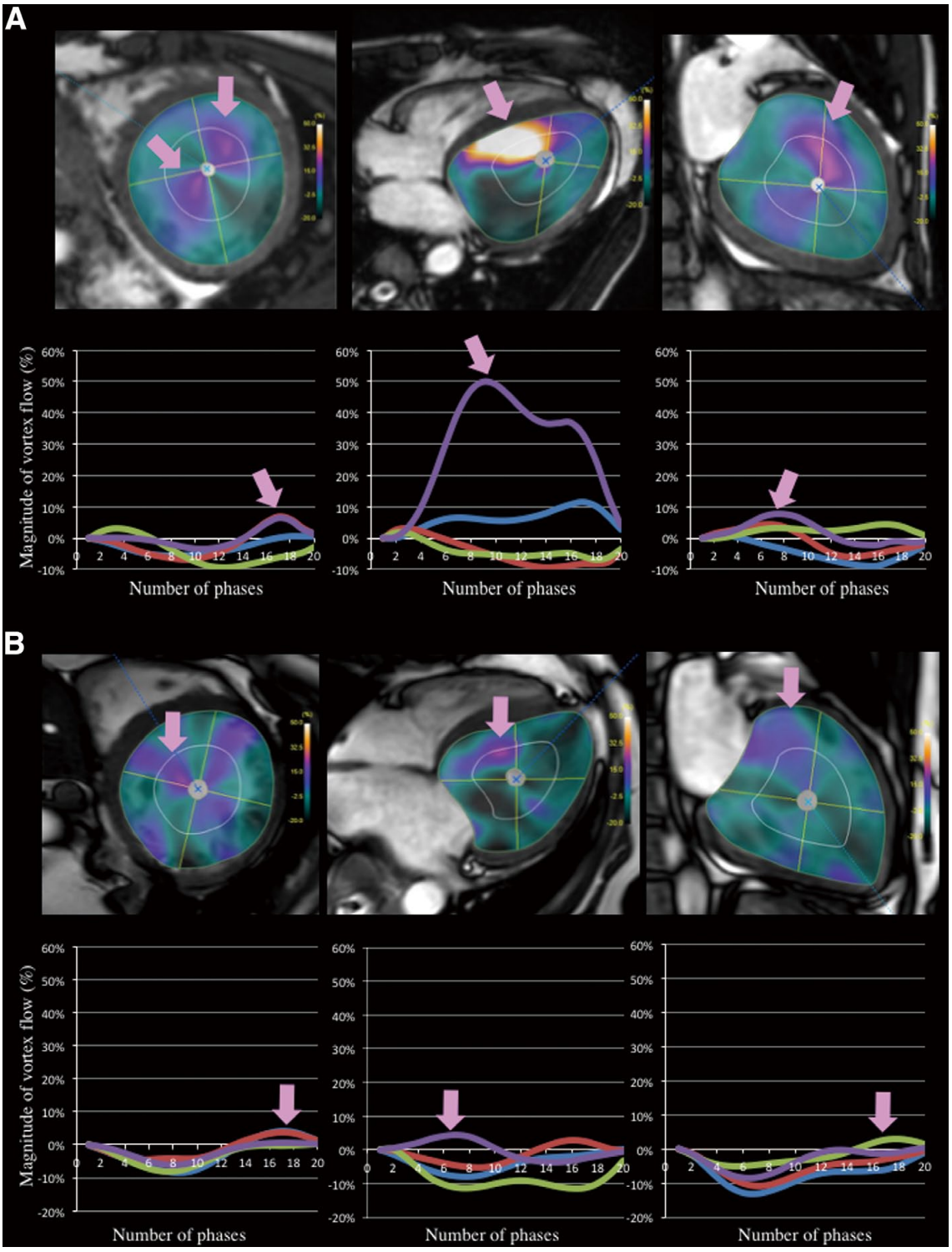

Figure 2. Vortex flow (VF) map and time curves of VF on the (**Left**) short-axis (SA), (**Center**) 4-chamber and (**Right**) long-axis (LA) images. Time curves of the VF were divided into 4 sections. Purple line, VF of septum (SA and 4-chamber) or basal (LA) segment. Red line, VF of the anterior (SA and LA) or apex (4-chamber) segment. Green line, VF of the lateral (SA and 4-chamber) or apex (LA) segment. Blue line VF of the inferior (SA and LA) or basal (4-chamber) segment. Arrow, maximum VF (MVF). (**A**) A man in his 30 s with dilated cardiomyopathy (DCM) who was a cardiac resynchronization therapy (CRT) responder. He spent 6.6 years without hospitalization for heart failure (HF) after CRT implantation. His summed MVF and left ventricle ejection fraction (LVEF) were 64.7% and 9.8%, respectively. Electrocardiogram (ECG) showed sinus rhythm, complete right bundle branch block (CRBBB), and QRS duration of 160 ms at the same time. (**B**) A man in his 60 s with DCM who was a CRT non-responder. He was hospitalized due to acute decompensated HF 5 months after CRT implantation. His summed MVF and LVEF were 7.6% and 18.5%, respectively. ECG showed sinus rhythm, intraventricular conduction disturbance, and QRS duration of 136 ms.

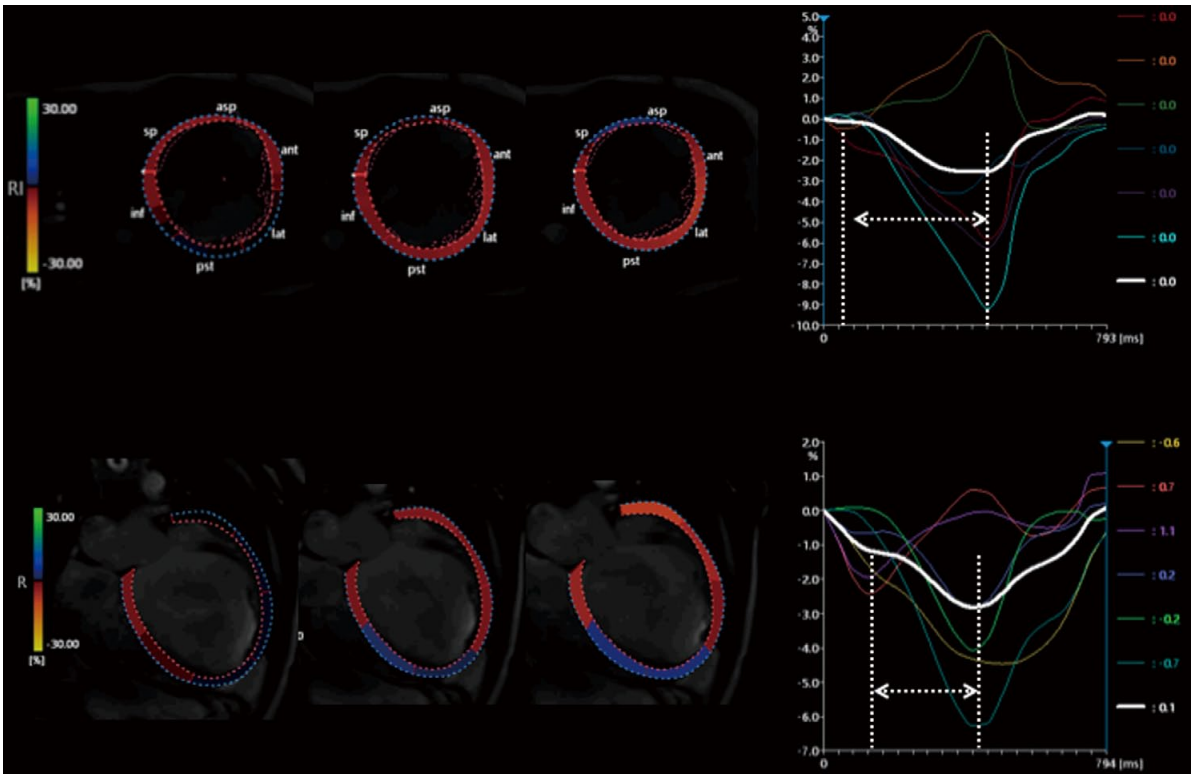

Figure 3. Feature tracking of cardiac magnetic resonance imaging (CMR-FT). Left ventricular (LV) (**Upper row**) short-axis and (**Lower row**) 4-chamber cine images ere used for analysis of LV dyssynchrony. CMR-FT semi-automatically tracks the contours of the endocardium and epicardium throughout a cardiac cycle. The LV was divided into 6 segments. The times to peak strain for the septal and lateral walls were obtained from (**Right side**) time curves of circumferential and longitudinal strain.

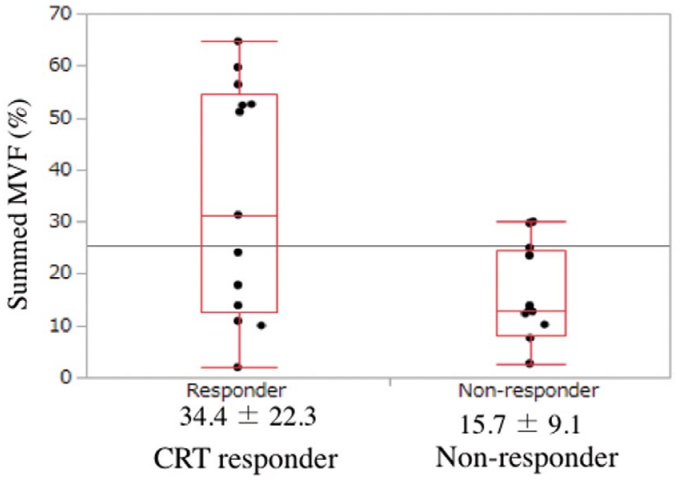

Figure 4. Summed maximum vortex flow (MVF) in cardiac resynchronization therapy (CRT) responders vs. non-responders (P<0.05). Horizontal line, maximum and minimum; ends of box, median; whiskers, upper quartile and lower quartile.

between the anteroseptum and posterolateral wall from QRS onset to maximum strain ratio was calculated, and a time difference >130 ms was defined as positive for intraventricular dyssynchrony.

Statistical Analysis

Continuous data are expressed as mean±SD. Comparisons of MVF, age, LVEDV and LVESV between the CRT group and LVEF ≥40% group were performed using the Mann-Whitney U-test. Comparison of MVF, age, QRS duration time, brain natriuretic peptide, LVEF, and LVEDV between

Table 2. Subject Characteristics vs. CRT Response

	CRT responders (n=12)	Non-responders (n=13)	P-value
Clinical characteristics			
Age (years)	56.0±15.7	62.2±16.4	0.32
Sex (male)	12 (100)	12 (92.3)	0.25
NYHA I/II/III	1/4/7	0/7/6	0.32
Paroxysmal AF	1 (8.3)	3 (23.1)	0.3
QRS duration (ms)	155.0±42.1	146.2±35.2	0.56
CLBBB	6 (50)	4 (30.8)	0.33
Baseline medication			
ACEI/ARB	12 (100)	13 (100)	1
β-blockers	11 (91.7)	13 (100)	0.22
Aldosterone inhibitors	8 (66.7)	8 (61.5)	0.79
Diuretics	9 (75.0)	12 (92.3)	0.23
Laboratory data			
BNP (pg/mL)	560.7±830.3	504.3±484.6	0.51
Echocardiography			
IVMD (ms)	46.9±36.1	23.1±10.5	0.1
STRSDI (ms)	172.6±141.2	160.8±100.9	1
MRI parameters			
LVEF (%)	15.6±8.8	16.7±7.1	0.72
LVEDV (mL)	339.6±165.4	259.9±151.1	0.19
Circumferential temporal delay (ms)	82.0±70.4	57.8±67.9	0.32
Longitudinal temporal delay (ms)	40.6±56.3	15.7±37.8	0.2
Summed MVF (%)	34.4±22.3	15.7±9.1	0.039*

Data given as mean±SD or n (%). ACEI, angiotensin-converting enzyme inhibitor; ARB, angiotensin II receptor blocker; BNP, brain natriuretic peptide; CLBBB, complete left bundle branch block; IVMD, interventricular wall motion delay; MRI, magnetic resonance imaging; STRSDI, speckle tracking radial strain delay index. Other abbreviations as in Table 1.

Table 3. Univariate Indicators of CRT Response

Parameter	OR	95% CI	P-value
NYHA	1.45	0.36–5.77	0.6
Paroxysmal AF	0.25	0.01–2.33	0.23
QRS duration	1	0.99–1.03	0.49
CLBBB	1.71	0.34–8.68	0.51
LVEDV	1	1.00–1.01	0.21
IVMD	1.02	0.99–1.05	0.1
STRSDI	1	0.99–1.01	0.82
Circumferential temporal delay (CMR-FT)	1.01	0.99–1.02	0.37
Longitudinal temporal delay (CMR-FT)	1.01	0.99–1.03	0.19
Summed MVF	1.07	1.01–1.14	0.0092*

*P<0.05. CMR-FT, cardiac magnetic resonance imaging-feature tracking. Other abbreviations as in Tables 1,2.

CRT responders and non-responders was also performed using the Mann-Whitney U-test. Comparison of the number of participants positive for LV dyssynchrony, who were male, had atrial fibrillation (AF), or had complete LBBB (CLBBB) and medication use between the CRT group and LVEF ≥40% group, and between CRT responders and non-responders, was carried out using Fisher's exact test. The correlation between summed MVF and the other parameters was analyzed using Pearson's correlation coefficient. Logistic regression analysis was performed to evaluate the factors associated CRT response. Receiver operating characteristic (ROC) curve analysis was performed to determine the optimal cut-off of summed MVF for the prediction of CRT response. Survival curves of patient subgroups were created using the Kaplan-Meier method to clarify the time-dependent, cumulative cardiac death and ADHF-free rate and were compared using the log rank test. P<0.05 was considered to indicate statistical significance. These analyses were performed using JMP version 9.0 (JMP, Cary, NC, USA).

Results

VF and LVEF

There was no significant difference in gender, NYHA classification, or presence of paroxysmal AF between the CRT

and LVEF ≥40% groups. All MVF were significantly greater for the CRT group than for the LVEF ≥40% group, although summed MVF had a higher level of significance (**Table 1**).

VF and CRT Response

Patients with DCM were classified as responders (n=12) or non-responders (n=13) during the follow-up period of 38.4±25.5 months (median, 30 months) after CRT. Four of 13 non-responders died: 2 patients died of HF, 1 died of sustained ventricular tachycardia, and 1 had sudden cardiac death. Five patients were hospitalized for ADHF, and 1 of 5 patients had a left ventricle assist device (LVAD) implanted. The average time to onset of ADHF was 16.8±15.3 months (median, 13 months) and LVAD was implanted 72 months after CRT implantation. The other 4 non-responders had an increase of LVESV <15% after CRT.

Summed MVF was significantly greater for CRT responders than for non-responders (34.4±22.3% vs. 15.7±9.1%, P<0.05; **Figure 4**).

The standard CRT predictors, such as AF, QRS durations, CLBBB, and LV dyssynchrony index on echocardiography did not differ between the CRT responders and non-responders. Circumferential dyssynchrony derived from CMR-FT was observed significantly more frequently in CRT responders than in non-responders (**Table 2**).

The predictive factors for CRT response were identified on univariate logistic regression analysis. Summed MVF had the strongest association with CRT response (OR, 1.07; 95% CI: 1.01–1.14; P=0.0092; **Table 3**).

On ROC analysis the optimal cut-off of summed MVF of 31.3% could predict CRT response with an area under the curve of 0.74, a sensitivity of 0.58, and a specificity of 1.00.

Patients with summed MVF ≥31.3% had a significantly higher cardiac death and ADHF hospitalization-free rate than those with summed MVF <31.3% (log-rank value=4.51, P=0.034, **Figure 5**).

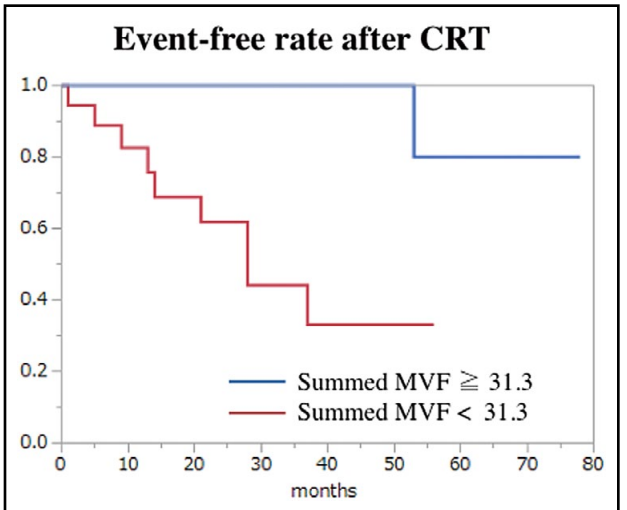

Figure 5. Cardiac death and acute decompensated heart failure hospitalization event-free curves after cardiac resynchronization therapy (CRT) according to summed maximum vortex flow (MVF) ≥31.3% (blue) or <31.3% (red) (P=0.034).

VF and LV Dyssynchrony

Circumferential and longitudinal temporal delay times for the responder group were 82.0±70.4 and 40.6±56.3 ms, and those for the non-responder group were 57.8±67.9 and 15.7±37.8 ms, respectively. There was no significant difference in either of the temporal delay times between the responder and non-responder groups (P=0.32 and 0.20, respectively). Temporal delay time and summed MVF had moderate correlation (circumferential temporal delay, r=0.56, P=0.0035; longitudinal temporal delay, r=0.59, P=0.0020).

Discussion

This is the first trial using VFM with conventional cine CMR in LV analysis in patients with HF. Previous studies using VFM have succeeded in visualization of blood flow in the dilated right atrium in adult patients after Fontan operation.[2,3] The 4-D flow MRI or contrast echocardiography characterize blood motion in the LV using vertical flow dynamics,[15–18] but there has never been an easy or useful imaging method for visualization of blood flow on 2-D cine MRI (**Supplementary Movie**; **Supplementary Figure**). The VF software was originally used to quantify myocardial strain analysis for cine-tagging imaging based on voxel and feature-tracking methods, and its principle is the ratio of each voxel movement towards circumferential direction. Eriksson et al noted that intracardiac LV blood flow consists of 4 components: direct flow; retained inflow; delayed ejection flow; and residual volume.[16] Components other than residual volume consisted of linear flows, and only residual volume was a swirling flow in the LV. Further, delayed ejection flow and residual volume in severely dilated LV cause increase of kinetic energy loss, leading to heart overload. Our proposed VF targets on slow flow or stagnation along the LV wall out of mainstreams, which is considered to be a quantification of the residual volume with parts of retained inflow and delated ejection flow.

On VFM analysis, VF in the LV was associated with efficiency of LV ejection, and patients with HF and LVEF <40% had a significantly greater MVF than patients with LVEF >40%. Patients with DCM and a high MVF have better response to CRT than those without a high MVF. Interestingly, we found a moderate association between greater VF and LV mechanical dyssynchrony. The greater VF was highly asymmetrical and was often seen along the endocardium of an akinetic wall (**Figures 1**,**2**). Asymmetry has been classically related to the geometry of mitral and non-coaxial flow orientation along the ventricular LA.[19] The present results suggest the importance of the interaction of the vortex with the ventricular wall. We speculate that heterogeneous LV contraction and regional dyskinesis cause localized stagnation and the intermixing of slow and rapid flows in dilated LV. This makes an inhomogeneous magnetic field leading to dark flow phenomena; eventually it is seen as a VF. In the CRT group, the mean summed MVF for 4 patients who died was 21.9%, which was lower than that in the patients who survived (mean, 26.8%). This suggests that patients with a greater VF may have a better response to CRT therapy than patients with small VF. At the end-stage of DCM, myocardial fibrosis progresses in the entire LV, and LV wall movement become diffusely weak and akinetic.[20] VF cannot be established due to severe myocardial damage, relating to CRT non-response. On logistic regression analysis only summed MVF was significantly related to CRT response. No other dyssynchrony index is associated with CRT response.[21–24] Finally, summed MVF

may be the best predictor of CRT response. In a previous echographic particle imaging velocimetry (Echo-PIV) study, CRT responders had a more uniform vortex formation in the LV during CRT-ON as compared with CRT-OFF, and non-responders had a chaotic vortex formation in the LV during CRT-ON and -OFF.[25] VFM analysis might be successful in quantifying localized stagnation and the intermixing of slow and rapid flows due to asymmetric LV wall motion. We think that this phenomenon is similar to the chaotic vortex formation during CRT-OFF in the Echo-PIV study. VFM analysis is clinically useful if it can identify CRT responders and non-responders before CRT implantation.

The intraventricular vortex dynamics may be considered as potential indicators of various heart diseases.[26] During early diastolic filling and atrial contraction, blood flow crossing the mitral valve is directed towards the LV posterolateral wall, generating a vortex moving towards the apex. This helps the redirection of blood toward the LV outflow tract and promotes the conservation of kinetic energy from diastole into systole.[27,28] The physiological vortex formation is the result of the synergy of wall dynamic forces in an asymmetrical cavity of suitable volume. The vortex structures may increase ejection efficiency by conserving the momentum of blood built up during filling.[29] Finally, vortices may contribute to blood mixing inside the ventricle, avoiding stasis.[30]

Reduced VF in the right atrium after Fontan operation has been reported to be associated with the development of late phase complications in VFM studies.[2,3] VFM allows the evaluation of large recirculating flows in the dilated right atrium of Fontan circulation, which is characterized by relative low velocities. Recent echocardiography,[31,32] computational,[33] and phase-contrast CMR[15,17] studies have described intraventricular flow energetic properties in patients with normal and dilated hearts. With regard to pixel movement on 2-D cine CMR, the present VF is different to the vortex formation with the previous methods.[2,3] Patients with LVEF >40% had greater VF than patients with LVEF <40%. This is consistent with the observation in a recent color-Doppler echocardiography study of a greater vortex in the LV in patients with DCM, compared with normal subjects.[32]

With regard to the repeatability of the VF measurement, the present study has not been verified because we analyze the conventional 2-D cine images backwards. Also, accuracy of VF analysis with the 4-D MRI technique is much better than that of the 2-D technique, but the aim of the present study was to assess a simple, easy, and user-friendly 2-D technique.

Study Limitations

The present study has several limitations. First, this was a retrospective, single-center cohort study, and the sample size was small. Second, VFM could not be used to analyze VF after CRT implantation because artifacts due to the cardiac device occurred frequently in the LV. Therefore, we could not prove the improvement of VF in CRT responders. Third, this study was limited to analyzing only patients with DCM. We did not investigate the relationship between CRT response and VF in patients with other cardiomyopathies. Further studies are needed to clarify whether VF can be generalized as an indicator for predicting effectiveness of CRT.

Conclusions

On VFM analysis, the development of VF in LV interrupts efficient ejection in HF. MVF is the best predictor of CRT response in patients with DCM compared with other dyssynchrony parameters and biomarkers.

Acknowledgments

We thank Mr. Yamato Shimomiya of Ziosoft Co., Mr. Yuichiro Sano and Mrs. Seiko Shimizu of Canon Medical Systems Co. for technical assistance. This work was supported by the Japan Society for the Promotion of Science (JSPS) KAKENHI (16K10321).

Disclosures

The authors declare no conflicts of interest.

Conflicts of Interest

None.

References

1. Ponikowski P, Voors AA, Anker SD, Bueno H, Cleland JGF, Coats AJS, et al. ESC guidelines for the diagnosis and treatment of acute and chronic heart failure. *Eur Heart J* 2016; **37:** 2129–2200.
2. Ishizaki U, Nagao M, Shiina Y, Fukushima K, Takahashi T, Shimomiya Y, et al. Prediction of Fontan-associated liver disease using a novel cine magnetic resonance imaging "vortex flow map" in the right atrium. *Circ J* 2018; **82:** 2143–2151.
3. Shiina Y, Inai K, Takahashi T, Shimomiya Y, Ishizaki U, Fukushima K, et al. Vortex flow in the right atrium surrogates supraventricular arrhythmia and thrombus after atriopulmonary connection-type Fontan operation: Vortex flow analysis using conventional cine magnetic resonance imaging. *Pediatr Cardiol* 2018; **39:** 375–383.
4. Marsan NA, Bleeker GB, Ypenburg C, Ghio S, van de Veire NR, Holman ER, et al. Real-time three-dimensional echocardiography permits quantification of left ventricular mechanical dyssynchrony and predicts acute response to cardiac resynchronization therapy. *J Cardiovasc Electrophysiol* 2008; **19:** 392–399.
5. Nakamura M, Kido T, Kido T, Tanabe Y, Matsuda T, Nishiyama Y, et al. Quantitative circumferential strain analysis using adenosinetriphosphate-stress/rest 3-T tagged magnetic resonance to evaluate regional contractile dysfunction in ischemic heart disease. *Eur J Radiol* 2015; **84:** 1493–1501.
6. Yamasaki Y, Nagao M, Abe K, Hosokawa K, Kawanami S, Kamitani T, et al. Balloon pulmonary angioplasty improves interventricular dyssynchrony in patients with inoperable chronic thromboembolic pulmonary hypertension: A cardiac MR imaging study. *Int J Cardiovasc Imaging* 2017; **33:** 229–239.
7. Li W, Storey P, Chen Q, Li BS, Prasad PV, Edelman RR. Dark flow artifacts with steady-state free precession cine MR technique: Causes and implications for cardiac MR imaging. *Radiology* 2004; **230:** 569–575.
8. Storey P, Li W, Chen Q, Edelman RR. Flow artifacts in steady-state free precession cine imaging. *Magn Reson Med* 2004; **51:** 115–122.
9. Claus P, Salem AM, Pedrizzetti G, Sengupta PP, Nagel E. Tissue tracking technology for assessing cardiac mechanics principles, normal values, and clinical applications. *JACC Cardiovasc Imaging* 2015; **8:** 1444–1460.
10. Yonezawa M, Nagao M, Abe K, Matsuo Y, Baba S, Kamitani T, et al. Relationship between impaired cardiac sympathetic activity and spatial dyssynchrony in patients with non-ischemic heart failure: Assessment by MIBG scintigraphy and tagged MRI. *J Nucl Cardiol* 2013; **20:** 600–608.
11. Nagao M, Yamasaki Y, Yonezawa M, Kamitani T, Kawanami S, Mukai Y, et al. Geometrical characteristics of left ventricular dyssynchrony in advanced heart failure: Myocardial strain analysis by tagged MRI. *Int Heart J* 2014; **55:** 512–518.
12. Wiesbauer F, Baytaroglu C, Azar D, Blessberger H, Goliasch G, Graf S, et al. Echo Doppler parameters predict response to cardiac resynchronization therapy. *Eur J Clin Invest* 2009; **39:** 1–10.
13. Richardson M, Freemantle N, Calvert MJ, Cleland JG, Tavazzi L; CARE-HF Study Steering Committee and Investigators. Predictors and treatment response with cardiac resynchronization therapy

in patients with heart failure characterized by dyssynchrony: A pre-defined analysis from the CARE-HF trial. *Eur Heart J* 2007; **28:** 1827–1834.
14. Suffoletto MS, Dohi K, Cannesson M, Saba S, Gorcsan J 3rd. Novel speckle-tracking radial strain from routine black-and-white echocardiographic images to quantify dyssynchrony and predict response to cardiac resynchronization therapy. *Circulation* 2006; **113:** 960–968.
15. Eriksson J, Carlhall CJ, Dyverfeldt P, Engvall J, Bolger AF, Ebbers T. Semi-automatic quantification of 4D left ventricular blood flow. *J Cardiovasc Magn Reson* 2010; **12:** 9.
16. Eriksson J, Dyverfeldt P, Engvall J, Bolger AF, Ebbers T, Carlhäll CJ. Quantification of presystolic blood flow organization and energetics in the human left ventricle. *Am J Physiol Heart Circ Physiol* 2011; **300:** 2135–2141.
17. Eriksson J, Bolger AF, Ebbers T, Carlhall CJ. Four-dimensional blood flow-specific markers of LV dysfunction in dilated cardiomyopathy. *Eur Heart J Cardiovasc Imaging* 2013; **14:** 417–424.
18. Kheradvar A, Houle H, Pedrizzetti G, Tonti G, Belcik T, Ashraf M, et al. Echographic particle image velocimetry: A novel technique for quantification of left ventricular blood vorticity pattern. *J Am Soc Echocardiogr* 2010; **23:** 86–94.
19. Kheradvar A, Falahatpisheh A. The effects of dynamic saddle annulus and leaflet length on transmitral flow pattern and leaflet stress of a bileaflet bioprosthetic mitral valve. *J Heart Valve Dis* 2012; **21:** 225–233.
20. Assomull RG, Prasad SK, Lyne J, Smith G, Burman ED, Khan M, et al. Cardiovascular magnetic resonance, fibrosis, and prognosis in dilated cardiomyopathy. *J Am Coll Cardiol* 2006; **48:** 1977–1985.
21. Tayal B, Gorsan J 3rd, Delgado-Montero A, Marek JJ, Haugaa KH, Ryo K, et al. Mechanical dyssynchrony by tissue Doppler cross-correlation is associated with risk for complex ventricular arrhythmias after cardiac resynchronization therapy. *J Am Soc Echocardiogr* 2015; **28:** 1474–1481.
22. Yu CM, Hayas DL. Cardiac resynchronization therapy: State of the art 2013. *Eur Heart J* 2013; **34:** 1396–1403.
23. Neubauer S, Redwood C. New mechanisms and concepts for cardiac-resynchronization therapy. *N Engl J Med* 2014; **370:** 1164–1166.
24. Seo Y, Ito H, Nakatani S, Takami M, Naito S, Shiga T, et al. The role of echocardiography in predicting responders to cardiac resynchronization therapy: Results from J-CRT. *Circ J* 2011; **75:** 1156–1163.
25. Cimino S, Palombizio D, Cicogna F, Cantisani D, Reali M, Filomena D, et al. Significant increase of flow kinetic energy in "nonresponders" patients to cardiac resynchronization therapy. *Echocardiography* 2017; **34:** 709–715.
26. Sengupta PP, Pedrizzetti G, Kilner P, Kheradvar A, Ebbers T, Tonti G, et al. Emerging trends in CV flow visualization. *JACC Cardiovasc Imaging* 2012; **5:** 305–316.
27. Kilner PJ, Yang GZ, Wilkes AJ, Mohiaddin RH, Firmin DN, Yacoub MH. Asymmetric redirection of flow through the heart. *Nature* 2000; **404:** 759–761.
28. Pedrizzetti G, Domenichini F. Nature optimizes the swirling flow in the human left ventricle. *Phys Rev Lett* 2005; **95:** 108101.
29. Abe H, Caracciolo G, Kheradvar A, Pedrizzetti G, Khandheria BK, Narula J, et al. Contrast echocardiography for assessing left ventricular vortex strength in heart failure: A prospective cohort study. *Eur Heart J Cardiovasc Imaging* 2013; **14:** 1049–10609.
30. Toger J, Kanski M, Carlsson M, Kovacs SJ, Soderlind G, Arheden H, et al. Vortex ring formation in the left ventricle of the heart: Analysis by 4D flow MRI and Lagrangian coherent structures. *Ann Biomed Eng* 2012; **40:** 2652–2662.
31. Agati L, Cimino S, Tonti G, Cicogna F, Petronilli V, De Luca L, et al. Quantitative analysis of intraventricular blood flow dynamics by echocardiographic particle image velocimetry in patients with acute myocardial infarction at different stages of left ventricular dysfunction. *Eur Heart J Cardiovasc Imaging* 2014; **15:** 1203–1212.
32. Bermejo J, Benito Y, Alhama M, Yotti R, Martinez-Legazpi P, Del Villar CP, et al. Intraventricular vortex properties in nonischemic dilated cardiomyopathy. *Am J Physiol Heart Circ Physiol* 2014; **306:** 718–729.
33. Mangual JO, Kraigher-Krainer E, De Luca A, Toncelli L, Shah A, Solomon S, et al. Comparative numerical study on left ventricular fluid dynamics after dilated cardiomyopathy. *J Biomech* 2013; **46:** 1611–1617.

Supplementary Files

Supplementary Movie. Vortex flow mapping.

Please find supplementary file(s);
http://dx.doi.org/10.1253/circrep.CR-18-0024